

This is the author's final version of the contribution published as:

Colombero C., Comina C., Rocchietti D., Garbarino G.B., Sambuelli L. Ground penetrating radar surveys in the archaeological area of Augusta Bagiennorum: Comparisons between geophysical and archaeological campaigns (2021) Archaeological Prospection, DOI: 10.1002/arp.1855.

The publisher's version is available at:

<https://onlinelibrary.wiley.com/doi/full/10.1002/arp.1855>

When citing, please refer to the published version.

This full text was downloaded from iris-AperTO: <https://iris.unito.it/>

GPR surveys in the archaeological area of *Augusta Bagiennorum*: comparisons between geophysical and archaeological campaigns

Colombero C.¹, Comina C.², Rocchietti D.³, Garbarino G.B.⁴, and Sambuelli L.¹

¹ Politecnico di Torino, Dipartimento di Ingegneria dell'Ambiente, del Territorio e delle Infrastrutture, DIATI, Torino, Italy.

² Università degli Studi di Torino, Dipartimento di Scienze della Terra, DST, Torino, Italy.

³ Soprintendenza Archeologia belle arti e paesaggio per la città metropolitana di Torino, Italy.

⁴ Soprintendenza Archeologia belle arti e paesaggio per le province di Alessandria, Asti e Cuneo, Italy.

ABSTRACT

Geophysical methods, and particularly Ground Penetrating Radar (GPR), have been increasingly applied as a preliminary mapping tool to guide archaeological excavations. Direct comparisons between geophysical and archaeological features is however not always systematically performed given the different time spans, covered areas, acquisition and processing approaches of the surveys. A critical comparison between geophysical and archaeological results is here proposed on a test site within the archaeological area of *Augusta Bagiennorum* (NW Italy). Three rectangular sectors covering an area of approximately 2325 m² were investigated with high-density GPR profiles and compared with both historical and new archaeological excavations. The GPR amplitude and attribute analyses highlight the effectiveness of geophysical prospections in identifying buried linear (i.e. walls) and localized (e.g. pillars or columns) archaeological remains. The recent archaeological excavations fully confirm the interpretation of the GPR results. Historical archaeological trenches, filled with coarse material after the excavation, are also found to generate strong anomalies in the GPR amplitude, similar to the ones of the buried structures, but with irregular contours and oblique orientations with respect to Roman remains. The GPR prospections also highlight interesting buried elements in unexplored areas, supporting important archaeological interpretations about the spatial configuration of the Roman city. The results help to recognize sectors with significant and well-preserved buried remains that can be brought to light in the future to promote heritage conservation and enhancement at the site.

Keywords: GPR, archaeological prospection, *Augusta Bagiennorum*, texture attributes.

Short title: GPR surveys for archaeological prospection at *Augusta Bagiennorum*

Correspondence:

Chiara Colombero
Politecnico di Torino, DIATI
Corso Duca degli Abruzzi 24,
10129 Torino (TO), Italy.
Tel.: +39 011 090 7669
chiara.colombero@polito.it

1 INTRODUCTION

Between the available geophysical methods for archaeological prospection, Ground Penetrating Radar (GPR) is the most adopted for the high-resolution imaging of near-surface targets (Piro et al., 2003; Conyers & Leckebusch, 2010; Goodman & Piro, 2013; Trinks et al., 2018). With advances in software and imaging techniques, GPR data interpretation for archaeological prospection is evolving from the analysis of single 2D profiles to the reconstruction of 3D volumes, and to attribute analyses, better enabling the spatial tracing of the desired targets (Pipan et al., 1999; Nuzzo et al., 2002; Leckebusch, 2003; Zhao et al., 2015; Trinks & Hinterleitner, 2020). Between the large variety of possible attribute computations, the extraction of texture attributes from GPR data has been proven to provide clearer images of distribution, volume, and shape of potential archaeological targets and related stratigraphic units (e.g. Zhao et al., 2016). Texture attributes are commonly exploited for image processing, remote sensing and 2D-3D seismic reflection data analysis (e.g. Chopra & Alexeev, 2006) and can be used to further recognize the spatial organization of reflection amplitudes also in GPR data.

GPR has largely demonstrated its applicability and effectiveness for archaeological investigations over Roman remains (e.g. Neubauer et al., 2002; Linford, 2004; Yalçiner et al., 2009; Piro et al., 2017; Lockyear & Shlasko, 2017; Verdonck et al., 2020). Indeed, GPR data interpretation is favoured in this investigation context given the directionality of the targets to be imaged. Buried walls and structures show peculiar patterns related to the usually regular (i.e. perpendicular) construction approach of Roman urbanists. Nevertheless, the contrast in electromagnetic properties (i.e. mainly dielectric permittivity) between buried remains and surrounding soil is site dependent. Therefore, successful GPR imaging and its applicability should be evaluated on the basis of the available geological information. In important archaeological sites, subjected to different archaeological investigations during the time, traces and remains from former excavations could also partially alter the obtainable geophysical image. Therefore, the increase in case histories reporting on the comparison between GPR images and archaeological evidence in well documented sites would be a benefit to better understand potentialities and pitfalls of GPR with respect to direct excavations (e.g. Colombero et al., 2020).

With these aims, high-density GPR surveys were acquired in the archaeological area of *Augusta Bagiennorum*, a well-known and important Roman site located in Piedmont Region, NW Italy (Figure 1). The geophysical results are here critically compared to the outcomes of historical and new archaeological excavation campaigns.

2 STUDY SITE AND HISTORICAL FRAMEWORK

The foundation of *Augusta Bagiennorum* took place after 27 BC and the site was permanently occupied only after the end of the century. To the present knowledge, the area was within the territory of the *Bagienni*, a Ligurian population on friendly terms with Rome, settled in the SW of the actual Piedmont Region.

The site is located on a plateau (340 m a.s.l.), between Tanaro and Stura di Demonte Rivers, characterized by terraced alluvial deposits (sands and gravels with pebbles) covered by a thin layer of fine-grained agricultural soil. The absence of specific geomorphological constraints or pre-existing settlements allowed for the application of a particularly rigorous urban planning scheme, exemplary compared to the canons developed in the Augustan Age (Preacco, 2014). The urban layout extended for approximately 21 hectares, divided by orthogonal road axes that formed a network of square (70 m × 70 m) or rectangular (80 m × 100 m) blocks. The city was abandoned in the early Middle Ages and remembered only through sparse textual sources.

Since its initial rediscovery at the end of 19th century, the site underwent detailed archaeological studies and excavations. Between 1892 and 1909, two local scholars, Giuseppe Assandria and Giovanni Vacchetta, extensively explored the site with non-stratigraphic excavation trenches and topographical surveys that led to the unequivocal identification of the Roman city and to the delineation of the urban perimeter (Assandria & Vacchetta, 1925). Many important public buildings were identified, such as the theatre (1, in Figure 1) and the main city temple, identified as the *Capitolium* (2, in Figure 1). These buildings are still visible nowadays, thanks to later excavations and restorations carried out between 1950 and 1970 (unearthed remains in red in Figure 1). Most of the archaeological trenches from the first excavations of Assandria & Vacchetta (1925) were conversely buried just after the delineation of the city plan and the orthogonal road pattern (buried remains in blue in Figure 1).

Among these buried features, the southern part of the civil *basilica* (3, in Figure 1) is of particular interest. It is indeed inserted in a central urban sector, between the area of the theatre and the *Capitolium* and shows interesting planimetric and structural aspects that still need to be better understood, especially in relation to the adjacent *forum* (4, in Figure 1).

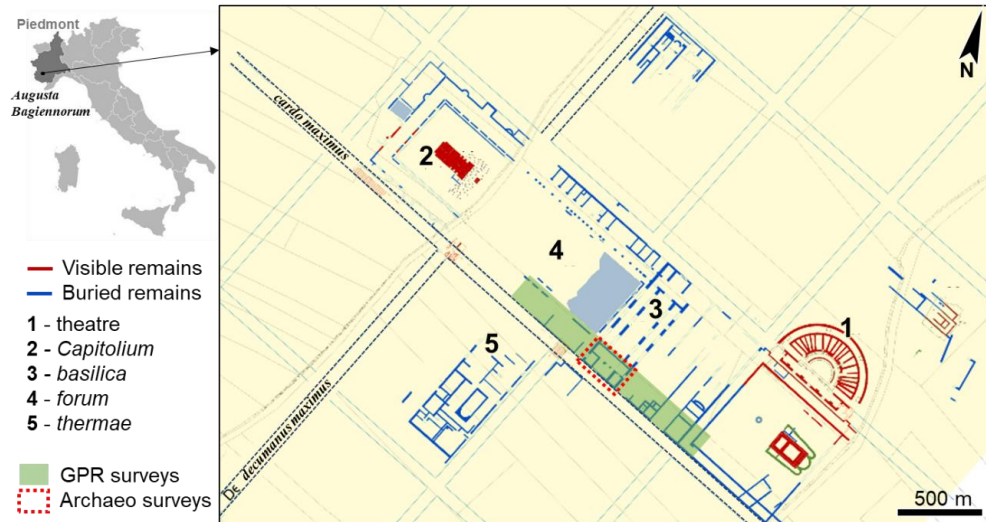


Figure 1. The archaeological area of *Augusta Bagiennorum*, detailed map of the city plan and remains from past archaeological surveys (modified after Assandria & Vacchetta, 1925) and location of the sectors investigated in the present paper. The inlet shows the geographic location of the area, in NW Italy.

The *forum* is undoubtedly the most interesting element of *Augusta Bagiennorum* urban layout. In literature, it is considered an exemplary case of bipartite *forum* (Maggi, 2007; Gros, 2007; or tripartite if the *basilica* is considered as a separate third element), with a clear distinction between civil and religious spaces on the two sides of *decumanus maximus* (i.e. the urban road segment running across the *forum*, orientated towards the Alpine passes, Figure 1). The sacred area occupied the NW part of the *forum*, around the *Capitolium*. To the SW of the *decumanus maximus*, monumental buildings surrounded the civil *forum* on three sides: the civil *basilica* on the short side, opposite to the *Capitolium*, and several *tabernae* on the long sides. A *porticus* probably ran around the *forum*, in front of the *tabernae*. Other important public buildings were connected to this central nucleus in a functional way, the *porticus post scaenam* of the theatre and a thermal complex (5, in Figure 1) located to the south of the *decumanus maximus*, reconstructed only through the trenches of the first excavations.

From the analysis of the available archaeological data, important aspects related to the *basilica* and *forum* are still unsolved: i) the intended use of the different rooms in the civil

buildings reconstructed by Assandria & Vacchetta (1925); ii) the articulation of the inner spaces of the *basilica* and its connections with the outside, iii) the expected, but unconfirmed, symmetry internal to the *forum*, with a *porticus* on the southern side, specular to the one suggested by Assandria & Vacchetta (1925) along the northern *tabernae*.

Augusta Bagiennorum is therefore an ideal site to increase the understanding of the urban topography of the minor centres of the Augustan Age and of their public areas. The already available data are particularly abundant, albeit acquired through non-stratigraphic trenches at the end of the 19th century (i.e. digging of localized trenches and interpolated information among these trenches) and therefore not completely exhaustive. Furthermore, the regularity and symmetry of the urban layout and the adherence to consolidated urban planning models allow for predictability even on parts of the city not directly explored by excavations. Other predisposing factors are the scarcity or absence of wall structures belonging to medieval or modern times, due to the early abandonment of the urban centre, and the modest soil cover on the crests of the buried walls (i.e. a few decimetres).

Therefore, geophysical acquisitions (green rectangles in Figure 1) and archaeological excavations (red dotted rectangle in Figure 1) were carried out in the area between the *forum* and the *basilica* and are reported in the present paper. Particularly, GPR amplitude and textural attribute results are discussed in relation to both historical and newly executed archaeological excavations. These last aimed to identify possible phases of restoration or reuse of the Roman *basilica*, understand its internal structure and verify its spatial relationship with the adjacent square (*forum*), given the absence of evidence about the location of the accesses to the public building. The GPR results can also further guide future archaeological activities in the area and help to recognize sectors with significant and well-preserved buried remains that can be brought to light in the future, promoting heritage conservation and enhancement.

3 MATERIALS AND METHODS

3.1 GPR Surveys

Three rectangular sectors (S1 to S3 in Figure 2) were investigated through the GPR surveys in different times, from 2016 to 2019. The survey areas are expected to be located at the SW margins of the civil *basilica* and *forum*. Nowadays, there is no surface evidence

of the buried remains, even if a few freely accessible orthophotos of the archaeological park acquired in past years enable to roughly recognize linear buried features NE of the investigated sectors (e.g. Google Maps, Figure 2a). These peculiar signatures are probably due to the fact that the photos were acquired during a dry period (August 2017) with scarce vegetation cover and few traces of agricultural activity at the ground surface, which are now more pronounced and almost totally hide the archaeological traces. Their location and orientation correspond to buried remains (Figure 2b) already mapped by Assandria & Vacchetta (1925). Continuity and precise identification of the southern plan of these structures is therefore the main aim of the GPR surveys.

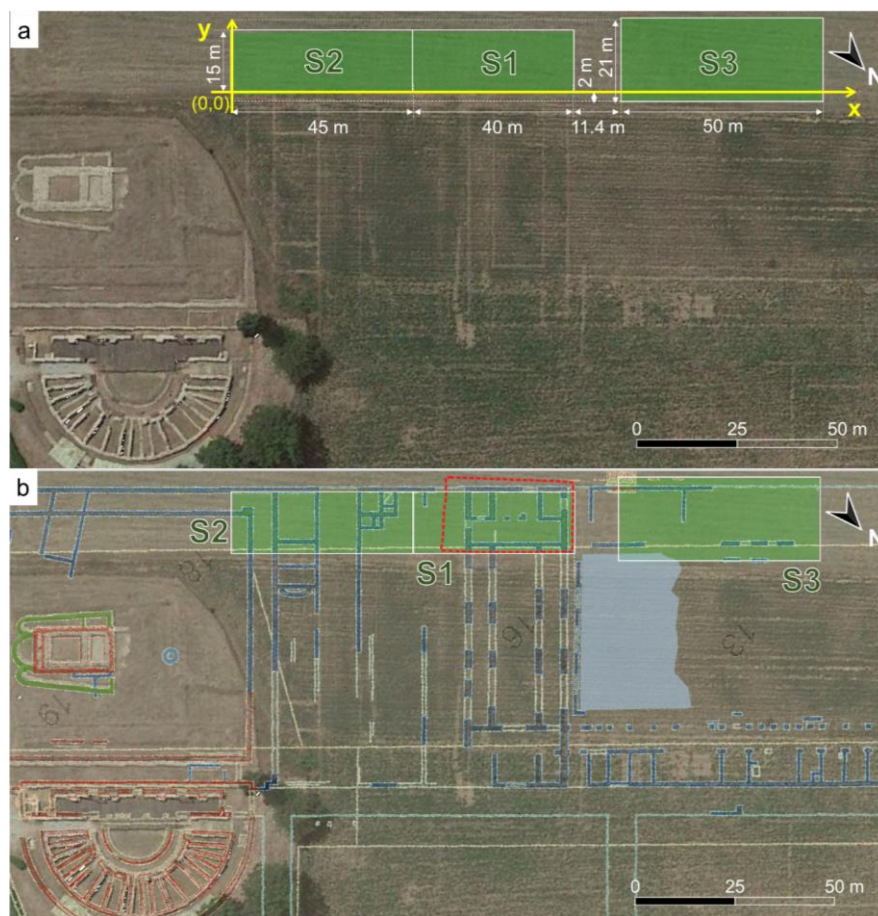


Figure 2. GPR survey areas (green rectangles, S1 to S3; local reference system in yellow) overlapped to (a) the orthophoto of *Augusta Bagiennorum* archaeological park (modified from Google Earth, August 2017) and (b) the map of the remains (see Figure 1) reconstructed after Assandria & Vacchetta (1925). The location of the new archeological excavation is highlighted with a red dashed line in (b).

Specifically, S1 is located at the southern edge of the *basilica*. S2 is the south-eastern continuation of the previous sector and can disclose further buried remains useful to identify the spatial relationships between the *basilica* and the discontinuous buildings

mapped in that area. S3 is located on the southern long side of the *forum*, to verify the internal symmetry and possibly discover the presence of a *porticus*, not mapped during the historical archaeological campaigns.

The x-axis of each investigated sector lays approximately on NW-SE direction (138° from N), the y-axis is perpendicular (Figure 2a). Meandering GPR profiles were acquired along the x-direction of each rectangle, with a 500-MHz GSSI antenna connected to a IDS K2 unit. A surveying cart with a wheel encoder (IDS Survey Wheel Kit WHE50) was used to drag the antenna along the investigated direction and allow correct trace positioning. The four corners of each rectangle were georeferenced using a RTK-GPS Topcon GRS-1 for further data spatial integration. Survey and acquisition parameters for each GPR campaign are reported in Table 1. After testing the effectiveness of GPR imaging in sector S1, with parallel profiles at 0.5-m distance, the profile spacing was reduced to 0.3 m for S2 and S3, to ensure a denser spatial sampling, more suitable for archeological reconstruction.

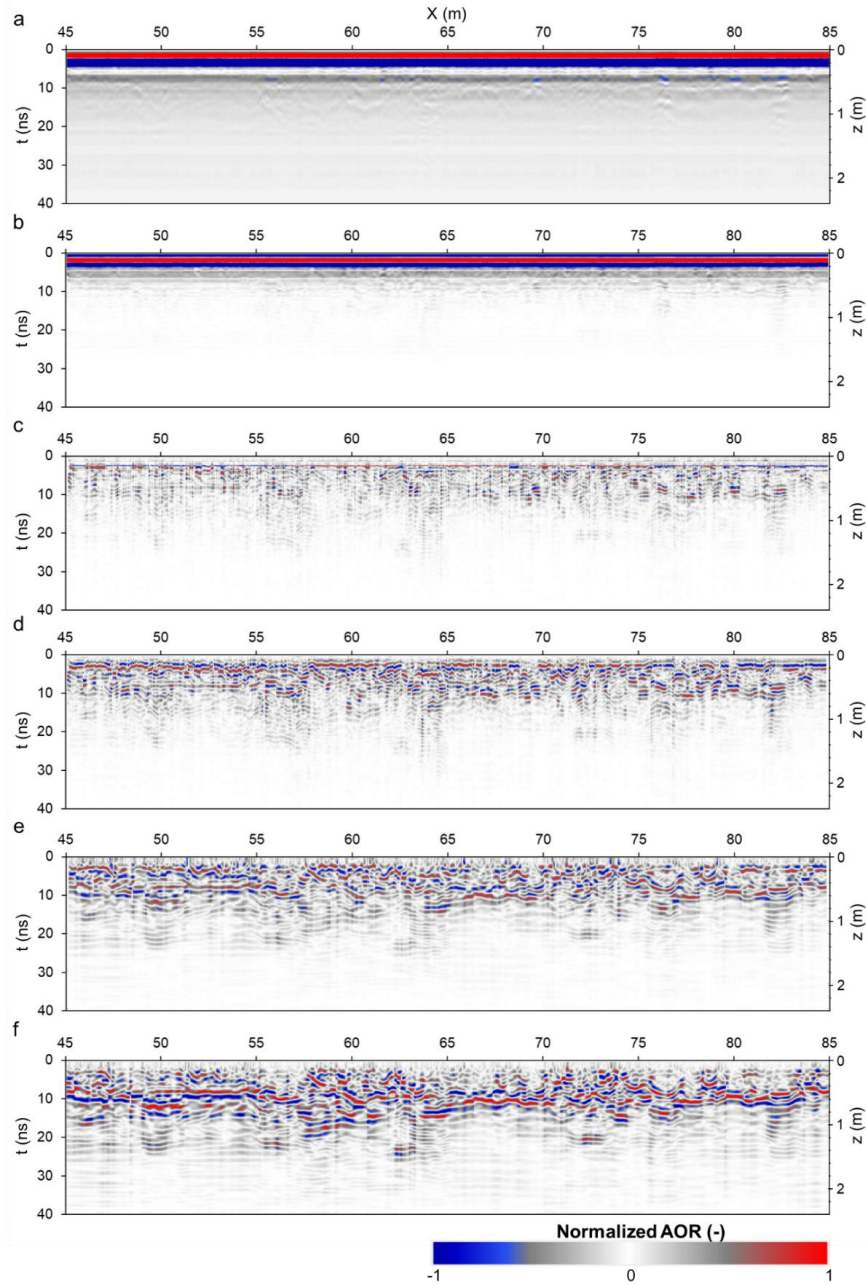
Table 1. GPR survey and acquisition parameters. Lx and Ly: x- and y-length of the investigated sectors S1 to S3. Δy: spacing between subsequent GPR profiles. The average number of traces along each profile is indicated in the sixth column. Δx: average spacing between the traces along each profile. The number of samples in each trace is reported in the last column.

	Lx (m)	Ly (m)	n. of profiles (-)	Δy (m)	n. of traces (-)	Δx (m)	Recorded length (ns)	n. of samples (-)
S1	40	15	31	0.5	635	0.06	50	512
S2	45	15	51	0.3	715	0.06	50	512
S3	50	21	71	0.3	780	0.06	80	1024

Raw radargrams acquired in the three sectors were processed in Reflexw (©Sandmeier geophysical research), with a common sequence (Figure 3), including:

- start time shift in correspondence of the main bang (i.e. air-ground reflection with the highest amplitude), to remove the signal delay and retrieve a correct travel time in the subsurface (Figure 3a);
- dewow, i.e. high-pass filtering to remove electronic low-frequency noise (Figure 3b);
- background removal, i.e. average trace subtraction to attenuate the horizontal clutter along the profiles (Figure 3c);
- band-pass filtering in the 180-720 Hz range, to attenuate noise outside the frequency band of interest (Figure 3d);

- 214 - diffraction stack, to collapse diffractions and back-propagate the reflections to their
- 215 real position (Figure 3e).
- 216 - time cut at 40 ns, common to all sectors, to create GPR data volumes with the same
- 217 time/depth.
- 218 - Manually designed gain to recover the amplitude of the deepest reflections (Figure
- 219 3f).



220 Figure 3. GPR processing sequence on a sample radargram (S1, southern trace): (a) start time
 221 moved, (b) dewowed, (c) back-ground removed, (d) band-pass filtered, (e) diffraction stacked, (f)
 222 compensated with a manual gain. All sections show the time axis already cut at 40 ns.
 223

Slight variations of the EM wave velocity between the different acquisitions were observed through the fitting of localized diffraction hyperbolas in the radargrams, likely as a consequence of the different soil moisture conditions in the survey dates. An average constant EM wave velocity of 0.12 m/ns was however considered for time-to-depth conversion. Processed radargrams were then assembled in their 3D spatial configuration (x, y, time/depth) in order to map and follow the spatial continuity of the GPR anomalies between the three sectors and have a direct comparison with excavation results.

Time-slices were extracted from the GPR data volume, with a vertical integration of 1 ns (half-length of the antenna period), to investigate the distribution of the amplitude of reflection (AOR) in maps parallel to the ground surface, i.e. time-slices corresponding to progressively increasing two-way times (twt), and thus to increasing depths of investigation.

To further strengthen the interpretation, texture attribute analysis was carried out on the processed radargrams, exploiting the built-in textural attribute algorithms available in the software Reflexw. Textural features can be extracted using 2D gray-level co-occurrence matrices (GLCM) depicting spatial relations between neighboring pixels or cells. The quantities adopted in the computation are n gray levels of the amplitude of reflection in each cell ($n=16$). The cell size was fixed to the average period of the EM signal along the time axis (i.e. 2 ns, corresponding to approximately 20 samples and 0.24 m), and 5 traces along the distance axis (approximately 0.30 m) of each radargram, to work on almost square pixels. The pixel size also corresponds to the profile spacing in S2 and S3, meaning approximately cubic cells of the 3D GPR data volume, in analogy with seismic reflection texture attribute analyses (e.g. Chopra & Alexeev, 2006). This discretization partially reduces the spatial resolution with respect to AOR radargrams and time slices, but remains suitable for the detection of the archeological remains and the heterogeneities in the surrounding material, improving the signal-to-noise ratio of the attribute estimation.

The complete algorithm description is reported in Zhao et al. (2016). In summary, for each cell a square GLCM is built ($n \times n$). Each element in the matrix contains the occurrence frequency of the n gray level in the surrounding of the cell. The GLCM matrix is then normalized in order to obtain at each position (i.e. row i , column j) the probability of occurrence $P_{i,j}$ of a specific gray level pattern.

Extracted attributes were:

- Textural uniformity, also referred to as Energy (Zhao et al., 2016), reflecting the overall uniformity of the amplitude distribution (Figure 4a), following:

$$Uniformity = \sum_{i=1}^n \sum_{j=1}^n P_{i,j}^2 \quad (1).$$

- Local homogeneity, quantifying the overall smoothness of the radargram (Figure 4b), following:

$$Homogeneity = \sum_{i=1}^n \sum_{j=1}^n \frac{1}{1+(i-j)^2} P_{i,j} \quad (2).$$

- Local dissimilarity, highlighting contrasts and local amounts of amplitude variations in the radargram (Figure 4c), following:

$$Dissimilarity = \sum_{i=1}^n \sum_{j=1}^n |i - j| P_{i,j} \quad (3).$$

Each of these attribute represents a certain image property (i.e. coarseness, texture complexity or contrast) without any redundancy in the obtained information (Chopra & Alexeev, 2006).

Textural attribute sections were finally assembled in 3D data volumes with the same approach used for the AOR data. Attribute maps parallel to the ground surface at different times/depths were used to evaluate the effectiveness of textural analyses in imaging the archaeological structures.

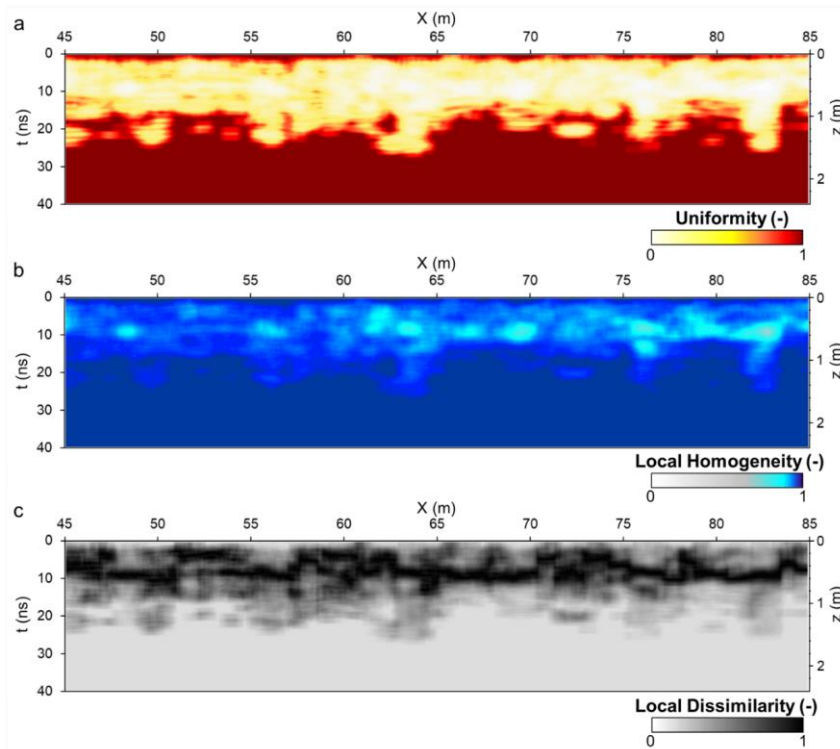


Figure 4. Textural attributes computed for sample radargram of Figure 1 (S1, southern trace): (a) energy or textural uniformity; (b) local homogeneity; (c) local dissimilarity.

3.2 Archaeological excavations

Although carried out and published with exceptional rigor and precision for the times, the 19th century non-stratigraphic trenches left unsolved doubts not only regarding the internal articulation of the *basilica* and its spatial relationship with the *forum*, but also about the dating and the possible structural changes or reuses of the building.

A new archaeological excavation was consequently performed at the southern edge of the *basilica* in 2019. It involved an approximately 18-m wide and 33-m long rectangular area, overlapping sector S1 (Figure 2b). The average depth of the excavation was around 1.2 m. After a shallow mechanical removal, the archaeologists removed the thin layer of soil covering the structures by trowel and the thicker layers by shovel and pickaxe. Once the area had been cleared up and the different stratigraphic units had been identified, georeferenced photogrammetric surveys were carried out with the use of drones. The different excavation levels were also precisely documented with drawings and detailed identification of the stratigraphic units.

4 RESULTS

4.1 GPR Surveys

Processed radargrams (Figure 3f) highlighted the presence of local anomalies in the amplitude of reflection from approximately 0.6 m depth. The location of these vertical features was often found to be consistent between subsequent profiles. To better enhance their lateral continuity, time slices of the AOR absolute value were therefore elaborated and are shown in Figure 5.

Starting from $twt=5$ ns (approximate depth of 0.3 m), linear anomalies with perpendicular orientations appear in the time slices of all the investigated sectors, likely indicating the presence of buried walls. The number, continuity and amplitude of these anomalies increase with depth, down to 1.5 m. Beside these regular alignments, anomalies with high AOR but with oblique or irregular orientation are also found. These anomalies are particularly visible and circled in Figure 5d both in S1 (around $x=73$ m and $y>6$ m) and in S2 (at $x<22$ m). In this sector, two oblique anomalies are clearly found within the buildings. The overall GPR amplitude in S1 seems globally higher in the top half of the sector. Other features appearing in the GPR time-slices are wide anomalies in the AOR in S2, between 20 m and 30 m, and in S1 between 62 m and 65 m along the x-direction,

and covering all the investigated distance along the y-axis (Figure 5d). In S3, regularly spaced localized anomalies are depicted along $y=0$ m. These last are located in front of the regular rooms highlighted between 8 m and 16 m along the y-direction. These GPR elements are likely indicating the presence of the *porticus* remains in front of the *tabernae*, along the southern side of the *forum*.

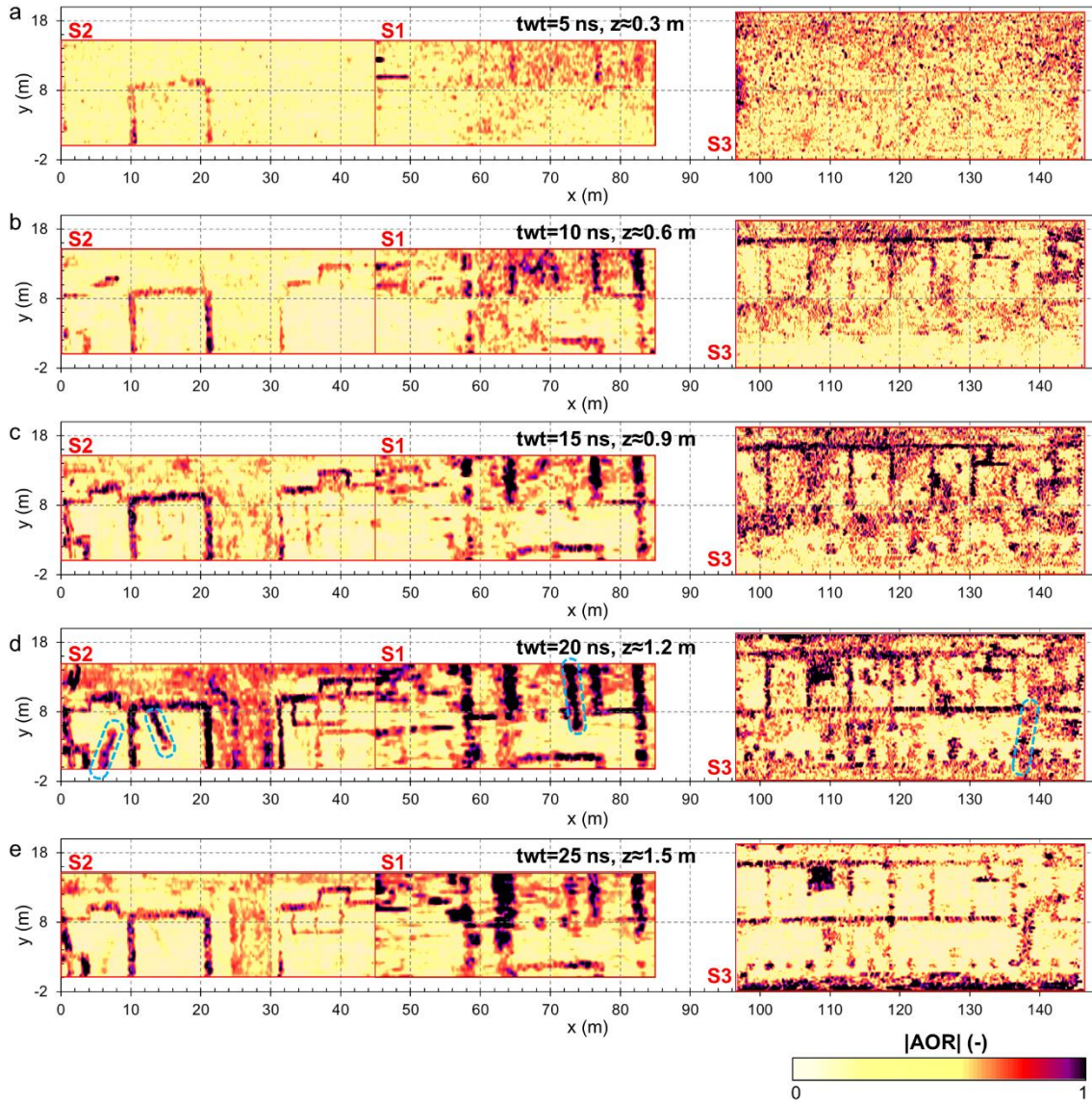


Figure 5. GPR time slices at increasing times (i.e. depths) from (a) to (e), for sectors S1 to S3 (AOR absolute values). Oblique anomalies are circled in blue in (d).

Time slices of the computed textural attributes are shown in Figure 6 to 8. The attribute analysis identifies the same features already depicted in the AOR time slices. However, textural attributes result in a clearer imaging of some patterns: the continuity of the buried walls is enhanced in most cases by local dissimilarity (Figure 8); the internal spaces of

the main rooms (e.g. in S2, $x > 30$ m) are better observable in local homogeneity time slices (Figure 7); the oblique anomalies are enhanced in the textural uniformity plots (Figure 6), while they look attenuated in the other textural attributes. Local dissimilarity is particularly effective in attenuating the effect of the oblique anomalies, while enhancing the archeological features of interest. It demonstrated also the best attribute to delineate the remains of the *porticus*, with columns or pillars at regularly spaced intervals. By contrast, the heterogeneities in the surrounding material, already depicted as wide areas with high AOR, are particularly evident in the uniformity time slices.

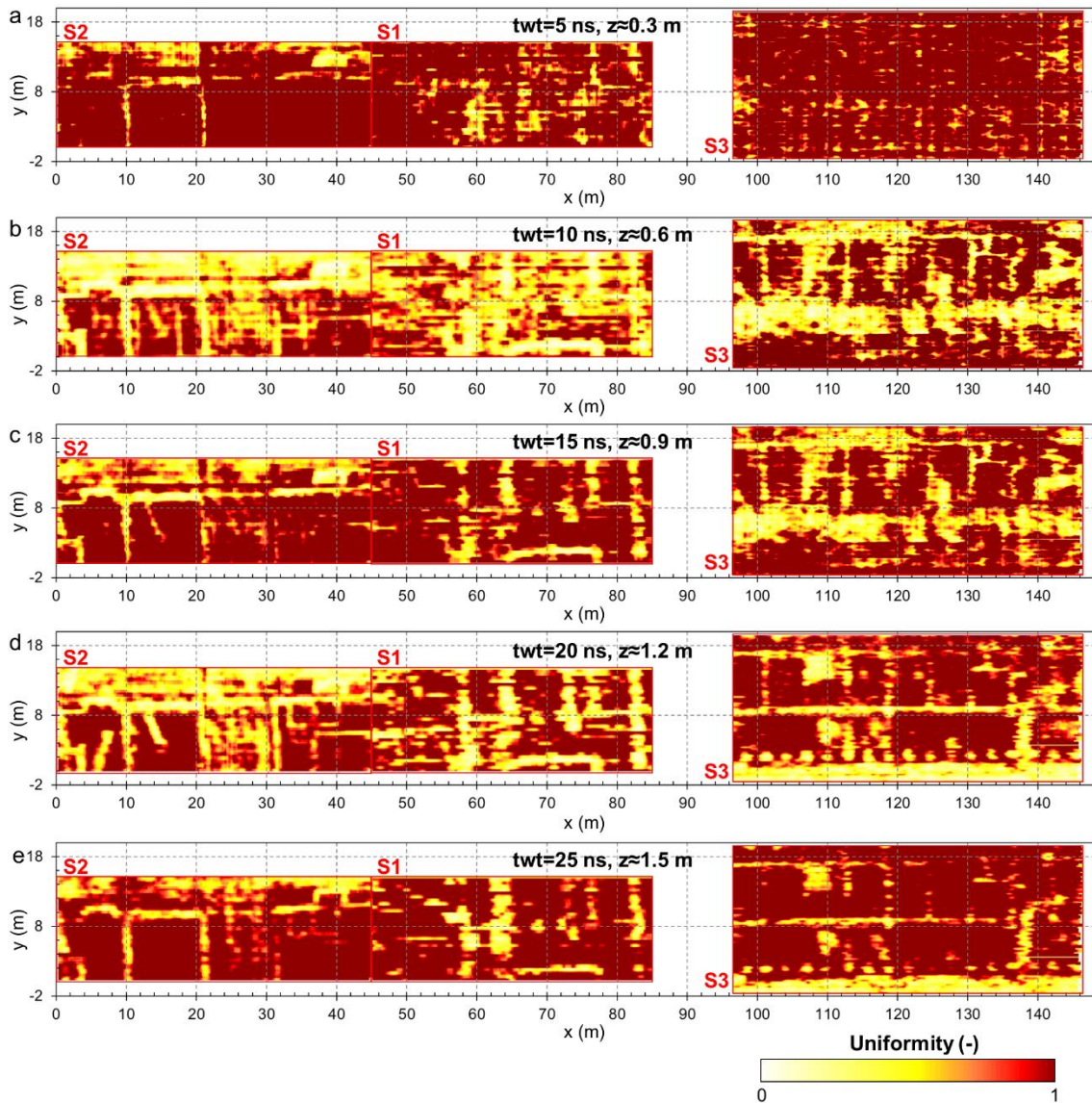


Figure 6. Textural uniformity time slices at increasing depths from (a) to (e), for sectors S1 to S3.

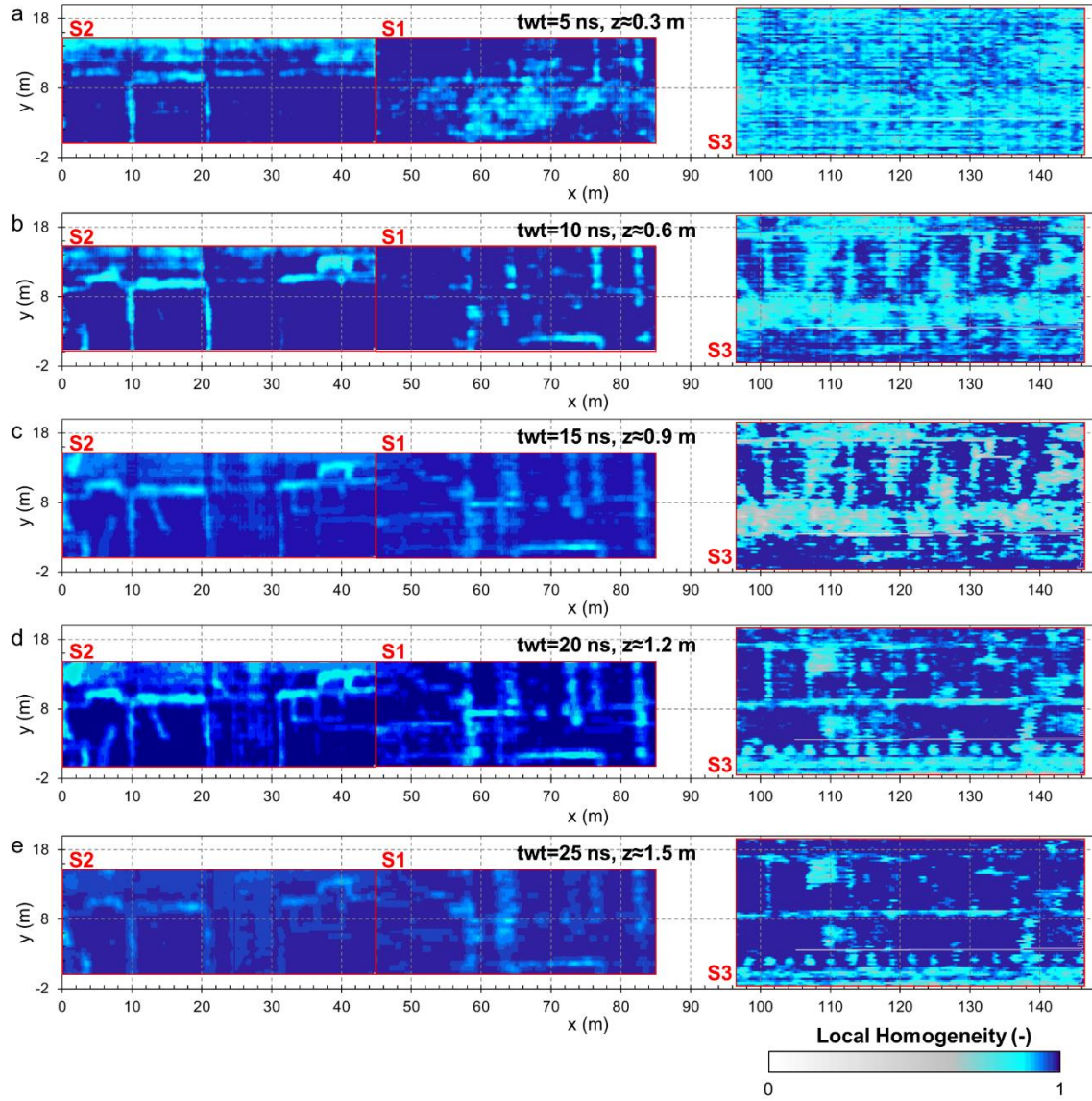


Figure 7. Local homogeneity time slices at increasing depths from (a) to (e), for sectors S1 to S3.

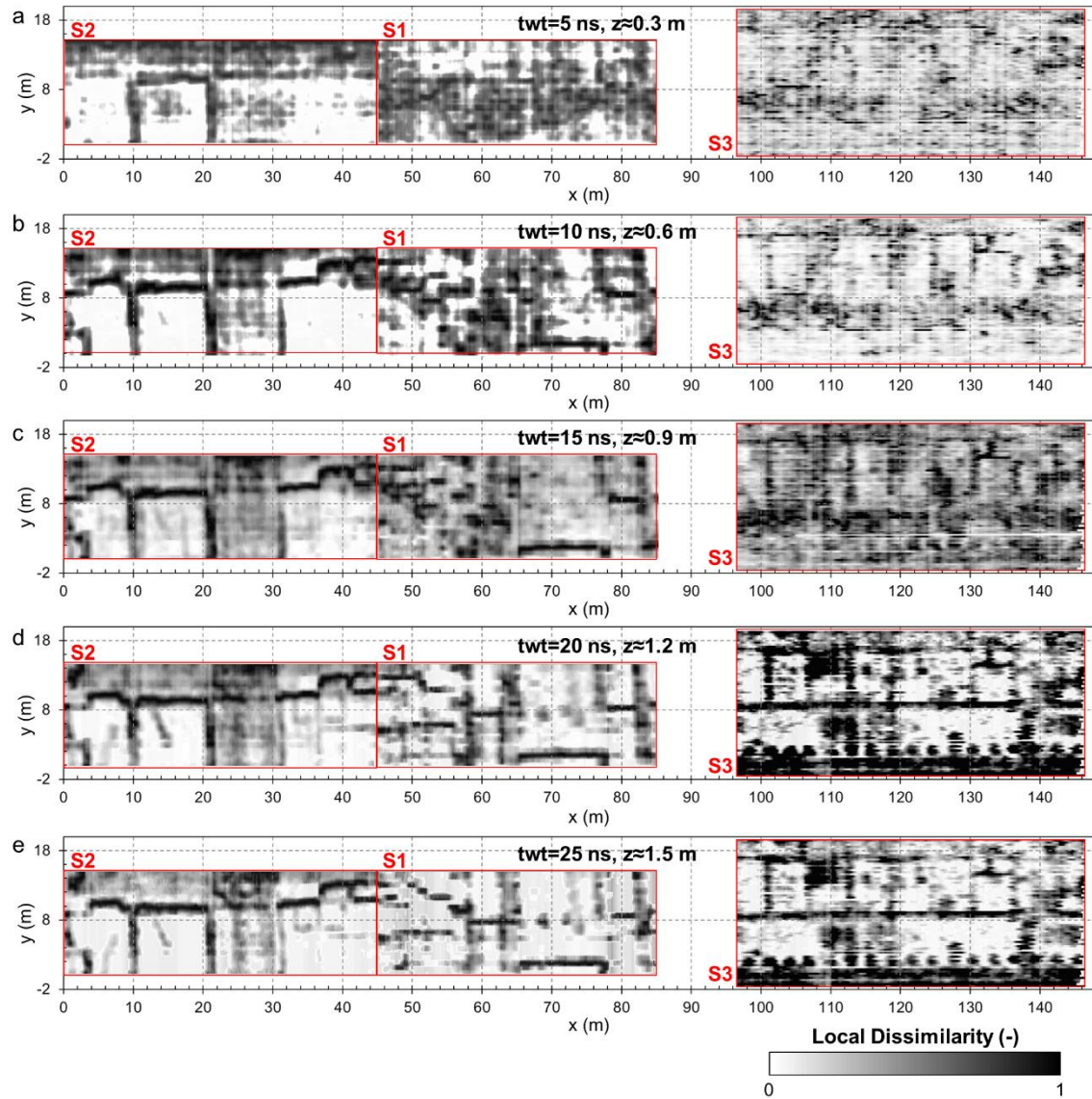


Figure 8. Local dissimilarity time slices at increasing depths from (a) to (e), for sectors S1 to S3.

4.2 Archaeological excavations

Structural evidence of the buried remains (Figure 9) started to emerge during archaeological excavations at the depth of approximately 0.3 m from the ground level. The walls showed lateral continuity from around 0.6-m depth, in agreement with the GPR results.



Figure 9. (a) Orthoimage of the archaeological excavation at the investigation depth of approximately 1.2 m. (b) Archaeological interpretation of the findings. The areas highlighted in yellow likely correspond to historical excavation trenches, filled by materials coarser than the surrounding areas.

The results confirm the existence of the civil *basilica*, featuring a rectangular plan with short straight sides along NW-SE direction. In the investigated southern sector, the *basilica* shows an articulation in three contiguous rooms probably facing the *ambulacrum* (i.e. open space surrounding the central room). The central room is characterized by a triple opening, given the presence of the foundations of two pillars, which stand in a slightly different location than that shown by the map of Assandria & Vacchetta (1925).

A few centimetres below ground level, the archaeological excavation revealed the collapsed roof of the *basilica* consisting of numerous tiles and many cover tiles laying on the soil surface, left after the removal of the floor tiles occurred in antiquity. At the current state of knowledge, the planimetric development of the *basilica*, or at least of its southern part, seems to have remained substantially unchanged since its foundation. At the corners of the structure, i.e. at the points of intersection between the perimeter walls and the internal ones, the walls are intentionally interrupted in the upper part (as visible in Figure 9a), likely to facilitate the insertion, on the continuous foundation wall, of other structural elements able to support the weight of the roof and carrying a decorative function at the same time. This constructive peculiarity was already observed during the excavations of the *Capitolium* (Preacco, 2014).

Besides these archaeological data, related to the Roman settlement, regular concentrations of river pebbles were also observed along specific locations (highlighted in Figure 9b). These features can be related to the filling of the old trenches or the rather regular cuts, probably attributable to the archaeological investigations of Assandria & Vacchetta (1925). These investigations were indeed filled with carefully selected material made of medium to large river pebbles, sometimes roughened, immersed in loose soil, probably collected during the same excavations and then thrown back into the trenches to facilitate the nearby agricultural works.

The archaeological investigation has removed all doubt regarding the chronology of the building thanks to the discovery of a votive deposit of three coins from the second half of the first century BC underneath some floor slabs, dating the *basilica* to the Augustan Age. The *basilica* underwent a long process of abandonment after losing its functionality that lasted probably until the fourth century AD, according to what can be observed for other public buildings in the city (Preacco, 2014). The building was deprived of all the ornamental elements, of which only a few fragments were recovered during the excavations, but also of all the other valuable construction materials that could be reused in other structures.

5 DISCUSSION

The GPR campaigns carried out in the *Augusta Bagiennorum* archaeological area proved able to effectively recognize and locate important buried remains. A detailed comparison between the GPR results and the past and recent archaeological findings is shown in

Figure 10. The reported GPR time slice corresponds to a depth of approximately 1.2 m (Figure 5d), close to the maximum depth of the most recent excavations. The location of the external walls of the *basilica* in the GPR results is in agreement with the previous map of the city (Figure 10a), although it was reconstructed only from local trenches, and with the recent archaeological findings (Figure 10b). An important variation with respect to the planimetric articulation of the *basilica*, interpreted on the basis of 19th century plan, is the absence of intermediate walls between the external perimeter and the internal wall delimiting the central space. This is a key feature, demonstrating the presence of an *ambulacrum* that likely completely surrounded the central area. This difference, already clear from the GPR results, was confirmed by the excavations.

Beside the walls of the southern edge of the *basilica*, other important elements were identified in the GPR results and interpreted thanks to the archaeological sounding. In particular, the oblique high-amplitude GPR anomalies were found to be precisely related to the coarser filling of trenches (Figure 10b) attributable to the archaeological investigations of Assandria & Vacchetta (1925). In all likelihood, the 19th century investigations were aimed primarily at the planimetric reconstruction of the buildings, since the pits and trenches identified are, in most situations, coinciding with the corners of the structures. The trenches showed AOR anomalies very similar to the walls, made up of similar materials. This underlines the effect that the disturbed stratigraphy, due to previous investigations, could have on the obtainable geophysical image and the need for a detailed documentation of the archaeological activities. Nevertheless, thanks to their irregular size and margins, oblique orientation with respect to the orthogonal city plan, and strong attenuation in the local dissimilarity time slices they could be discriminated in the GPR results. The abundant presence of trenches and coarser materials in the top half of the excavation rectangle (see Figure 9a) is also likely the cause of the general contrast in AOR between the two sectors, also highlighted in the textural uniformity results.

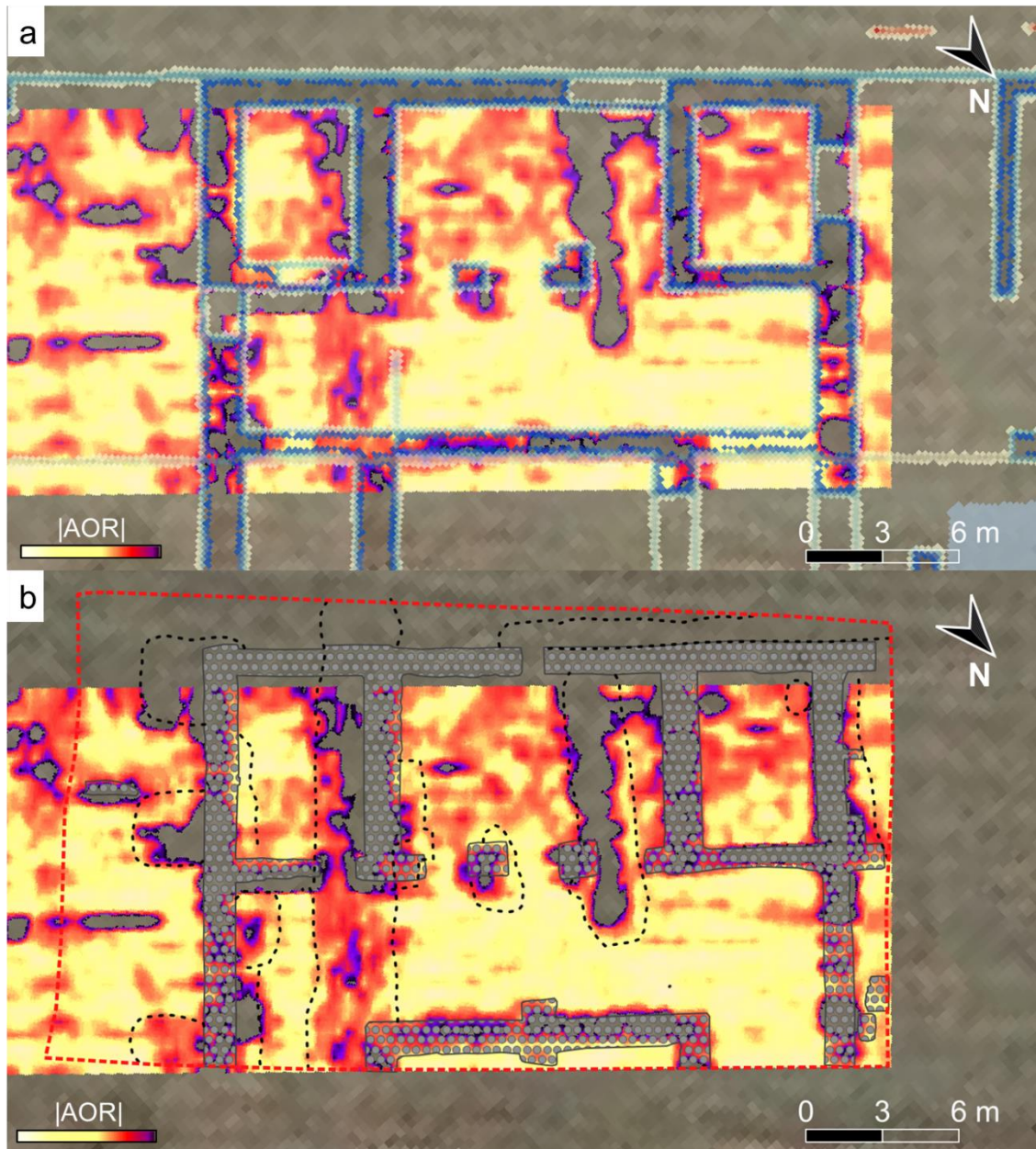


Figure 10. GPR results (time slice at 1.2-m depth) compared to: (a) the planimetric map of *Augusta Bagiennorum* reconstructed after Assandria & Vacchetta (1925), showing mapped remains in blue (now buried) and interpretations (in white); (b) a simplified scheme of the recent archaeological findings (from Figure 9b). The red dashed line delimits the excavation area. The dotted polygons refer to the location of the walls of the *basilica*. The black dashed lines correspond to the trenches filled with coarser pebbles after the work of Assandria & Vacchetta (1925).

Apart from the deep evidence of these main structures, the shallower GPR time slices are also able to depict the presence of sparse localized anomalies (see for example Figures 5c and 7c), probably related to the collapses of part of the roofs documented during the archaeological excavations.

A final comparison between the GPR results, the historical map of the remains and the site orthoimage over the *forum* and *basilica* area is reported in Figure 11. Despite minor shifts in the location, the continuity of the walls is confirmed by both surface evidence, historical data and geophysical prospections. A denser profile spacing in S1 would have possibly improved the wall delineation for the sector. However, given the good correspondence between GPR results and direct excavations in S1 sector, the GPR images can be interpreted with more confidence in the other two sectors, allowing for interesting archaeological considerations on the city plan to be performed even without the presence of further excavations. Further buried walls are found within S1 and S2, previously not mapped. The presence of a specular side in the *forum* is suggested from the GPR results in S3, with clear delineation of an alignment of regular *tabernae* and a parallel row of pillars towards the centre of the square.

All the above considerations and comparisons are shown on the AOR maps. The computed textural attributes revealed good imaging potential as well, but not adding particularly relevant improvements in the data interpretation for the present case history. The significant contrast between the remains and the surrounding alluvial deposits allowed indeed for a precise identification of the archaeological structures directly from the AOR maps. Given this contrast, only the local dissimilarity slices showed a partial imaging improvement for the archeological structures.



Figure 11. GPR results (time slice at 1.2-m depth) compared to the planimetric map of *Augusta Bagiennorum* reconstructed after Assandria & Vacchetta (1925) over the *forum* and *basilica* and the site orthoimage (Google Earth, 2017). Mapped remains (now buried) are shown in blue, interpretations are in white.

6 CONCLUSION

A critical comparison between geophysical and archaeological results was proposed in this work on a test site within the archaeological area of *Augusta Bagiennorum* (NW Italy). The site morphology presented no challenges for data acquisition, while data processing, visualization and interpretation required more efforts to obtain valuable information on the buried city plan. In particular, the interpretation of single radargrams offered poor characterization of the presence and continuity of buried structures, while time-slice amplitude and texture attribute results highlighted the effectiveness of GPR prospections in identifying buried linear (i.e. walls) and localized (e.g. pillars or column) archaeological remains. The recent archaeological excavations fully confirm the interpretation of the GPR results. In addition, the obtained subsurface images depict important elements also in areas not interested by excavations, enabling for further archaeological considerations about the spatial distribution and function of the civil spaces in the Roman city.

The case study underlined the importance of a specific comparison between the GPR results and archaeological data, for a more consistent data integration and more critical interpretations.

From the archaeological point of view, the combination of the GPR results and direct excavations has helped to clarify many structural aspects on the articulation of the spaces internal to the *basilica* and on the symmetry expected in the *forum*, with the identification of a *porticus* also on its southern side. However, due to the small size of the excavation, the dislocation of the openings of the *basilica*, towards the *forum* and the minor *decumanus* that flanked the building from the eastern side, is still an unsolved issue. With this respect, further investigations are necessary along the central portion of the building. Given the high quality of the obtained GPR results, further survey campaigns could be foreseen for this purpose and to check the state of preservation of other salient city remains (e.g. the south-eastern thermal complex). With respect to direct excavations, GPR would indeed allow to cover wide investigation areas with reduced times and costs. However, the agricultural use of the surrounding fields may limit GPR acquisition indeed even in absence of above ground vegetation, remains from agricultural activities (i.e. tractor tracks, corn crops) could compromise the GPR data quality particularly in the

shallow subsoil portion. To optimize data acquisition, multi-antenna arrays may help to reduce the acquisition time, preserving dense spatial sampling on the investigated areas.

Acknowledgments

The authors warmly thank Città di Bene Vagienna for site accessibility, permission and support to data acquisition. They are also grateful to Diego Franco for his support in the GPR campaigns.

REFERENCES

- Assandria, G., & Vacchetta, G. (1925). *Augusta Bagiennorum*. Planimetria generale degli scavi con cenni illustrativi. *Atti della Società Piemontese di archeologia e belle arti*, X, 2, 183–195.
- Chopra, S., & Alexeev, V. (2006). Applications of texture attribute analysis to 3D seismic data. *SEG Technical Program Expanded Abstracts 2005*, 767–770, 10.1190/1.2144439.
- Colombero, C., Elia, D., Meirano, V., & Sambuelli, L. (2020). Magnetic and radar surveys at *Locri Epizephyrrii*: A comparison between expectations from geophysical prospecting and actual archaeological findings. *Journal of Cultural Heritage*, 42, 147–157, 10.1016/j.culher.2019.06.012.
- Conyers, L.B., & Leckebusch, J. (2010). Geophysical archaeology research agendas for the future: some ground-penetrating radar examples. *Archaeological Prospection*, 17(2), 117–123.
- Goodman, D., & Piro, S. (2013). *GPR Remote Sensing in Archaeology* (pp. 1–233). Berlin, Germany: Springer.
- Gros, P. (2007). Organisation de l’espace et typologie monumentale, à propos de quelque forums “tripartis” de la Cisalpine. In L. Brecciaroli Taborelli (Ed.), *Forme e tempi dell’urbanizzazione nella Cisalpina (II secolo a.C. - I secolo d.C.)* (pp. 179–188). Atti delle Giornate di Studio (Torino, 4-6 maggio 2006), Borgo San Lorenzo.
- Leckebusch, J. (2003). Ground-penetrating radar: a modern three-dimensional prospection method. *Archaeological Prospection*, 10, 213–240.
- Linford, N. (2004). From hypocaust to hyperbola: Ground-penetrating radar surveys over mainly Roman remains in the UK. *Archaeological Prospection*, 11(4), 237–246.
- Lockyear, K., & Shlasko, E. (2017). Under the Park. Recent Geophysical Surveys at Verulamium (St Albans, Hertfordshire, UK). *Archaeological Prospection*, 24, 17–36. 10.1002/arp.1548.
- Maggi, S. (2007). Modelli e tipologie forensi in Cisalpina: alcune puntualizzazioni. In L. Brecciaroli Taborelli (Ed.), *Forme e tempi dell’urbanizzazione nella Cisalpina (II secolo a.C. - I secolo d.C.)* (pp. 283–286). Atti delle Giornate di Studio (Torino, 4-6 maggio 2006), Borgo San Lorenzo.
- Neubauer, W., Eder-Hinterleitner, A., Seren, S., & Melichar, P. (2002). Georadar in the Roman civil town *Carnatum*, Austria: An approach for archaeological interpretation of GPR data. *Archaeological Prospection*, 9, 135–156.

522 Nuzzo, L., Leucci, G., Negri, S., Carrozzo, M.T., & Quarta, T. (2002). Application of 3D
523 visualization techniques in the analysis of GPR data for archaeology. *Ann. Geophys.*, 45(2), 321–
524 338.

525 Pipan, M., Baradello, L., Forte, E., Prizzon, A., & Finetti, I. (1999). 2-D and 3-D processing and
526 interpretation of multi-fold ground penetrating radar data: a case history from an archaeological
527 site. *J. Appl. Geophys.*, 41, 271–292.

528 Piro, S., Goodman, D., & Nishimura, Y. (2003). The study and characterization of Emperor
529 Traiano's Villa (Altopiani di Arcinazzo, Roma) using high-resolution integrated geophysical
530 surveys. *Archaeological Prospection*, 10, 1–25.

531 Piro, S., Haynes, I., Liverani, P. & Zamuner, D. (2017). GPR investigation to map the subsoil of
532 the St. John Lateran Basilica (Rome, Italy). *Bollettino di Geofisica Teorica ed Applicata*, 58(4),
533 431–444.

534 Preacco, M.C. (2014). La città e i suoi monumenti alla luce delle recenti indagini archeologiche.
535 In *Augusta Bagiennorum. Storia e archeologia di una città augustea*, Torino: CELID, 99–121.
536

537 Trinks, I., Hinterleitner, A., Neubauer, W., Nau, E., Löcker, K., Wallner, M., Gabler, M.,
538 Filzwieser, R., Wilding, J., Schiel, H., Jansa, V., Schneidhofer, P., Trausmuth, T., Sandici, V.,
539 Ruß, D., Flöry, S., Kainz, J., Kucera, M., Vonkilch, A., Tencer, T., Gustavsen, L., Kristiansen,
540 M., Bye-Johansen, L.-M., Tønning, C., Zitz, T., Paasche, K., Gansum, T., & Seren, S. (2018).
541 Large-area high-resolution ground-penetrating radar measurements for archaeological
542 prospection. *Archaeological Prospection*, 25(3), 171–195.

543 Trinks, I., & Hinterleitner, A. (2020). Beyond Amplitudes: Multi-Trace Coherence Analysis for
544 Ground-Penetrating Radar Data Imaging. *Remote Sensing*, 12(10), 1538.

545 Verdonck, L., Launaro, A., Vermeulen, F., & Millett, M. (2020). Ground-penetrating radar survey
546 at Falerii Novi: A new approach to the study of Roman cities. *Antiquity*, 94(375), 705-723.
547 10.15184/aqy.2020.82

548 Yalçiner, C.C., Bano, M., Kadioglu, M., Karabacak, V., Meghraoui, M. & Altunel, E. (2009).
549 New temple discovery at the archaeological site of Nysa (western Turkey) using GPR method.
550 *Journal of Archaeological Science*, 36, 8, 1680–1689.

551 Zhao, W., Forte, E., Levi, S.T., Pipan, M., & Tian, G. (2015). Improved high-resolution GPR
552 imaging and characterization of prehistoric archaeological features by means of attribute analysis,
553 *Journal of Archaeological Science*, 54, 77–85.

554 Zhao, W., Forte, E. & Pipan, M. (2016). Texture attribute analysis of GPR data for archaeological
555 prospection, *Pure and Applied Geophysics*, 173, 2737–2751. 10.1007/s00024-016-1355-3